JOURNAL OF GEOPHYSICAL RESEARCH: ATMOSPHERES, VOL. 118, 1–10, doi:10.1002/jgrd.50475, 2013

Medicane risk in a changing climate

R. Romero[1] and K. Emanuel[2]

Received 15 January 2013; revised 2 May 2013; accepted 6 May 2013.

[1] Medicanes or "Mediterranean hurricanes" are extreme cyclonic windstorms morphologically and physically similar to tropical cyclones. Owing to their potential destructiveness on the islands and continental coastal zones, medicane risk assessment is of paramount importance. With an average frequency of only one to two events per year and given the lack of systematic, multidecadal databases, an objective evaluation of the long-term risk of medicane-induced winds is impractical with standard methods. Also, there is increasing concern about the way these extreme phenomena could change in frequency or intensity as a result of human influences on climate. Here we apply a statistical-deterministic approach that entails the generation of thousands of synthetic storms, thus enabling a statistically robust assessment of the current and future risk. Fewer medicanes but a higher number of violent storms are projected at the end of the century compared to present, suggesting an increased probability of major economic and social impacts as the century progresses.

Citation: Romero, R., and K. Emanuel (2013), Medicane risk in a changing climate, *J. Geophys. Res. Atmos.*, *118*, doi:10.1002/jgrd.50475.

1. Introduction

[2] Tropical-like cyclones of a few hundreds of kilometers in diameter occasionally evolve over the Mediterranean Sea [*Ernst and Matson*, 1983; *Rasmussen and Zick*, 1987; *Reale and Atlas*, 2001], posing a serious threat to any densely populated area found in the vicinity of their tracks. These storms have captured the attention of the research community and have been called medicanes (see Figure 1 for an example). Two basic facts in addition to its maritime origin reinforce the tropical analogy of a medicane: (i) its visual appearance in satellite images (as vigorous, highly concentric cloud bands wrapped around a central eye; e.g., *Tous and Romero* [2012]) and (ii) the essential roles of sea-to-air heat fluxes and latent heat release within the core of the storm as revealed by numerical simulations of real events [e.g., *Lagouvardos et al*., 1999; *Homar et al*., 2003; *Fita et al*., 2007; *Tous et al*., 2012]. Observations and simulations agree on the warm-core and small-scale nature of medicanes, which only exceptionally will induce hurricane-force winds (i.e., greater than 63 kt or 117 km/h) at the surface [e.g., *Fita et al*., 2007; *Moscatello et al*., 2008]. Both approaches also demonstrate the great difficulty in formulating a clear-cut distinction between medicanes and the broad spectrum of Mediterranean low-pressure systems, a significant fraction of which appear to be hybrid cyclonic storms that combine in different proportions the physical mechanisms of ordinary extratropical disturbances (e.g., frontal dynamics) with those described above. Some works conclude, for instance, that only 0.5 storms per year fulfill very strict medicane criteria in terms of cloud structure, degree of symmetry, size, and life span on satellite imagery [*Tous and Romero*, 2012]. When these criteria are relaxed to better account for the hybrid type of medicane, 1.5 storms per year are detected according to an informal register of events maintained by our group (see www.uib.es/depart/dfs/meteorologia/METEOROLOGIA/MEDICANES). An independent recent work [*Cavicchia*, 2013] established that about 1.6 genuine medicanes form over the Mediterranean basin per year. The present study deals with a geographical window somewhat larger than the Mediterranean waters by including the Black Sea and a sector of the Atlantic ocean (see Figure 8); therefore, for the purposes of a frequency normalization needed later on in our method, we will assume that two medicanes per year occur on average under the current climate.

[3] Some fundamental questions arise with regard to the actual medicane risk along the Mediterranean coasts: Are there favored locations for the development and maintenance of medicanes? How intense can they become? How could they react to human-induced global warming? Owing to the still short satellite history and the rarity of the phenomenon, these and other relevant questions are condemned to remain largely unanswered from a mere statistical analysis of the few existing records. The rarer the event, the more difficult it is to identify climatological patterns and long-term changes, simply because there are fewer cases to evaluate [*Frei and Schär*, 2001; *Klein Tank and Können*, 2003]. With regard to the effects of global warming, for the more abundant tropical cyclones, a substantial upward trend was reported in power dissipation (i.e., the sum over the lifetime

[1]Departament de Física, Universitat de les Illes Balears, Palma de Mallorca, Spain.
[2]Department of Atmospheric Science, Massachusetts Institute of Technology, Cambridge, Massachusetts, USA.

Corresponding author: R. Romero, Departament de Física, Universitat de les Illes Balears, Ctra. de Valldemossa km. 7.5, Palma de Mallorca ES-07122, Spain. (romu.romero@uib.es)

2169-897X/13/10.1002/jgrd.50475

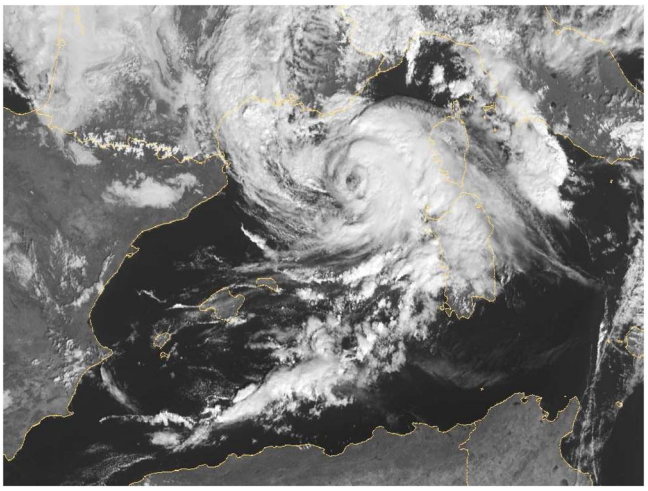

Figure 1. Satellite image of the medicane of 8 November 2011 in the western Mediterranean (source: EUMETSAT).

of the storm of the maximum surface wind speed cubed) over the last decades in the well-sampled North Atlantic and western North Pacific [*Emanuel*, 2005a; *Webster et al*., 2005]. This seems to be a consequence of the overall increase of tropical and subtropical sea surface temperature, which influences positively the so-called "potential intensity" (*PI*) of tropical cyclones through alterations of the surface energy flux [*Emanuel*, 1987; *Lighthill et al*., 1994; *Henderson-Sellers et al*., 1998]. *PI* expresses a balance between the mechanical energy available from the thermodynamic cycle that describes the steady state of an idealized tropical cyclone according to the air-sea interaction theory [*Emanuel*, 1986] and turbulent dissipation in the storm's atmospheric boundary layer. It is calculated from the environmental conditions as follows:

$$PI = \sqrt{\frac{C_k}{C_D}\frac{T_S - T_O}{T_O}\left(k_0^* - k\right)} \tag{1}$$

where T_S is the sea surface temperature, T_O the mean temperature at the top layer of the storm, k is the specific enthalpy of

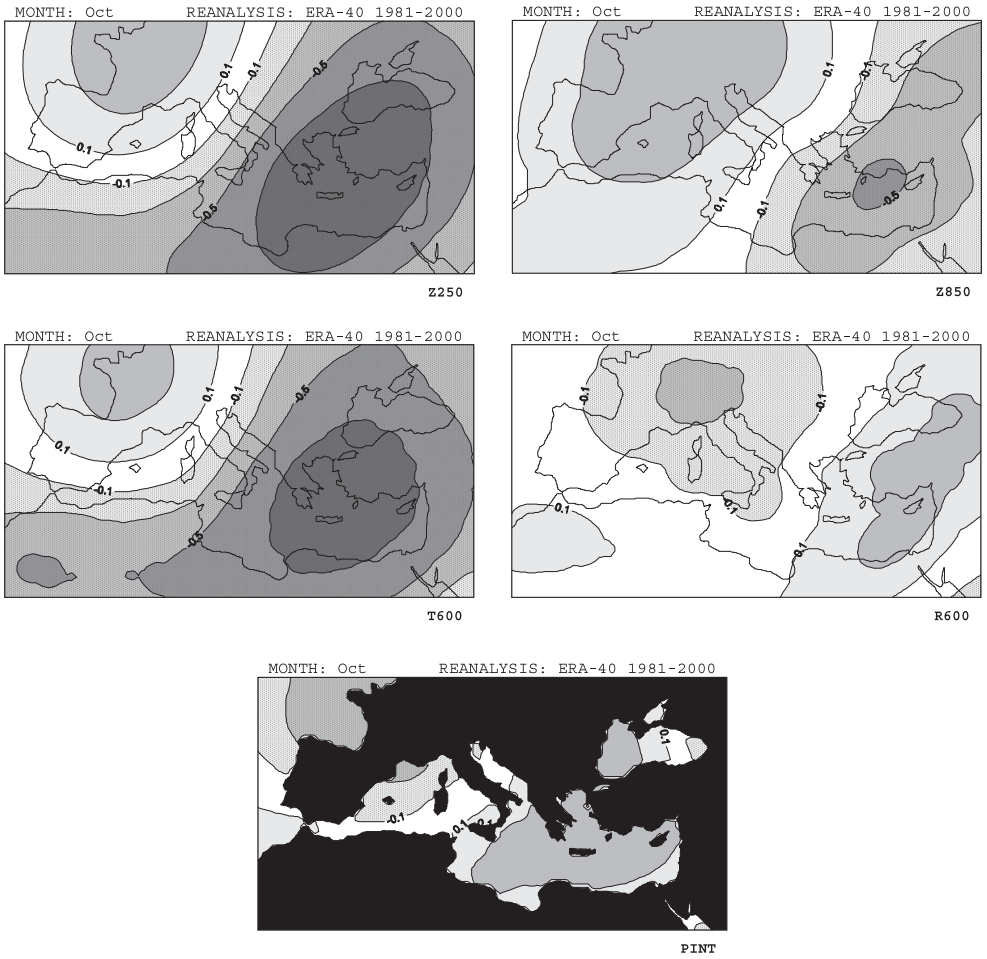

Figure 2. Depiction of the spatial-physical pattern for the first PC extracted from the October data of ERA-40 reanalysis. It represents a high/low (or low/high) dipole along the NW-SE direction on geopotential heights at 250 and 850 hPa (Z250 and Z850 maps) associated with warm/cold (or cold/warm) temperature at 600 hPa (T600 map), dry/moist (or moist/dry) midtroposphere (R600 map) and reduced/enhanced (or enhanced/reduced) potential intensity (PINT map). PC loadings are contoured at 0.2 interval, with negative areas shown as dotted.

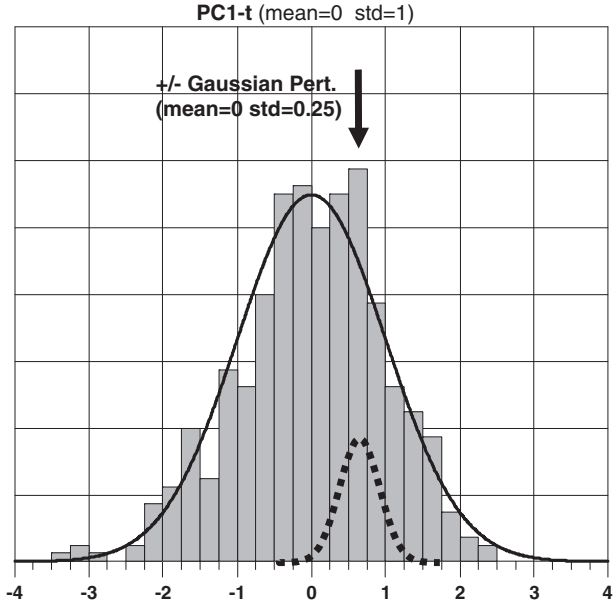

Figure 3. Frequency distribution of the first temporal PC extracted from the October data of ERA-40 reanalysis (bars). The distribution can be analytically adjusted to a normal distribution of mean 0 and standard deviation 1 (upper curve). The generation of synthetic 10 day synoptic states is based on Gaussian perturbations (lower curve) of observed PC values (arrow). See text for details.

air near the surface, k_0* is the enthalpy of air in contact with the ocean, assumed to be saturated with water vapor at ocean temperature, and C_D and C_k are the dimensionless transfer coefficients of momentum and enthalpy. The further increase of potential intensity during this century as projected by global climate models (GCMs) [*Emanuel*, 1987] is consistent with the increase in modeled storm intensities in a warmer climate [*Knutson and Tuleya*, 2004]. In contrast, no significant signal beyond natural variability has been detected in tropical cyclone global frequency over the past several decades [*Webster et al*., 2005], and research on possible future changes seems to offer ambiguous results with regard to increases or decreases in the total number of storms [*Henderson-Sellers et al*., 1998; *Royer et al*., 1998; *Sugi et al*., 2002].

[4] First attempts to evaluate medicane risk and its possible changes have been undertaken in recent years based on two different perspectives. The first approach examined the spatial and temporal variability of large-scale parameters (e.g., *PI* or derived quantities) indicative of the meteorological environments in which medicanes occur [*Tous and Romero*, 2012]. Unfortunately, these environmental proxies behave as necessary but not sufficient ingredients for the genesis of medicanes, and similar or even greater threshold values are found in ordinary cyclonic situations. Therefore, the utility of this approach is limited to providing only a general sense of the potential risk and its evolution. This type of analysis predicted an overall decrease in the future occurrence of medicane-prone meteorological situations. The second method consists of detecting and tracking symmetric warm-core cyclonic disturbances generated in nested climatic simulations. With this technique, *Gaertner et al*. [2007] found an enhanced future risk of severe medicane development using an ensemble of nine regional climate models (RCMs) covering the 1961–1990 and 2071–2100 time slices. The recent work of *Cavicchia* [2013] found a reduction of about 40% in the number of medicanes by the end of the century using a high-resolution RCM forced by a single global model. Owing to the high computational cost, this technique is limited by the horizontal resolutions used, which do not usually allow the RCMs to resolve the vast majority of medicanes as we know them today (i.e., small-scale vortices with very detailed inner region dynamics), and by the production of too few climate realizations as to permit an adequate and complete sampling of the probability distribution function of storms.

[5] Here we devise an alternative risk assessment method taking advantage of the statistical-deterministic approach developed by the second author and his team in the context of the long-term wind risk associated with tropical cyclones [*Emanuel et al*., 2006; *Emanuel*, 2006; *Emanuel et al*., 2008]. This approach generates thousands of synthetic storms with low computational cost, thus enabling a statistically robust assessment of the spatial-temporal risk function, in the form, for instance, of geographical distributions of return periods for extreme winds. By using GCM transient climate simulations instead of reanalyses as input data, the capabilities of this technique can be expanded to account for the expected effects of global warming.

2. Generation of Synthetic Medicanes

2.1. Summary of the Original Method

[6] In the original synthetic storm generation method, long-term records of tropical cyclone development are used to construct a space-time probability density of storm genesis over the great ocean basins [*Emanuel et al*., 2006]. Random draws from this distribution are used to initiate synthetic storm tracks. (An alternative method developed by *Emanuel et al*. [2008] randomly seeds the basin with weak warm-core cyclones.) Randomly varying synthetic time series of tropospheric mean winds are then generated which, however, have monthly mean, variances, and covariances that rigorously conform to climatological statistics from reanalysis or GCM data and which also conform to the power spectrum of geostrophic turbulence. Once created, these synthetic time series of tropospheric mean flow are used to generate synthetic storm tracks, making use of the observation that tropical cyclones move with a weighted mean environmental flow of the troposphere, plus a correction for the so-called "beta effect" owing to the Earth's curvature (the Beta and Advection Model; *Marks* [1992]). With this technique, it is easy to generate a very large number of storm tracks. Dynamical conditions along these tracks (e.g., vertical wind shear) are extracted from the synthetic winds, while other necessary thermodynamical parameters (e.g., potential intensity) are taken from the monthly climatologies interpolated to the storm position. Finally, a simple but accurate deterministic tropical cyclone intensity model, involving both atmospheric and oceanic elements [*Emanuel*, 1995], is run over each track to produce synthetic time series of storm intensity, including the radial distribution of wind. By this means, an accurate probability distribution of hurricane winds at any point can be generated.

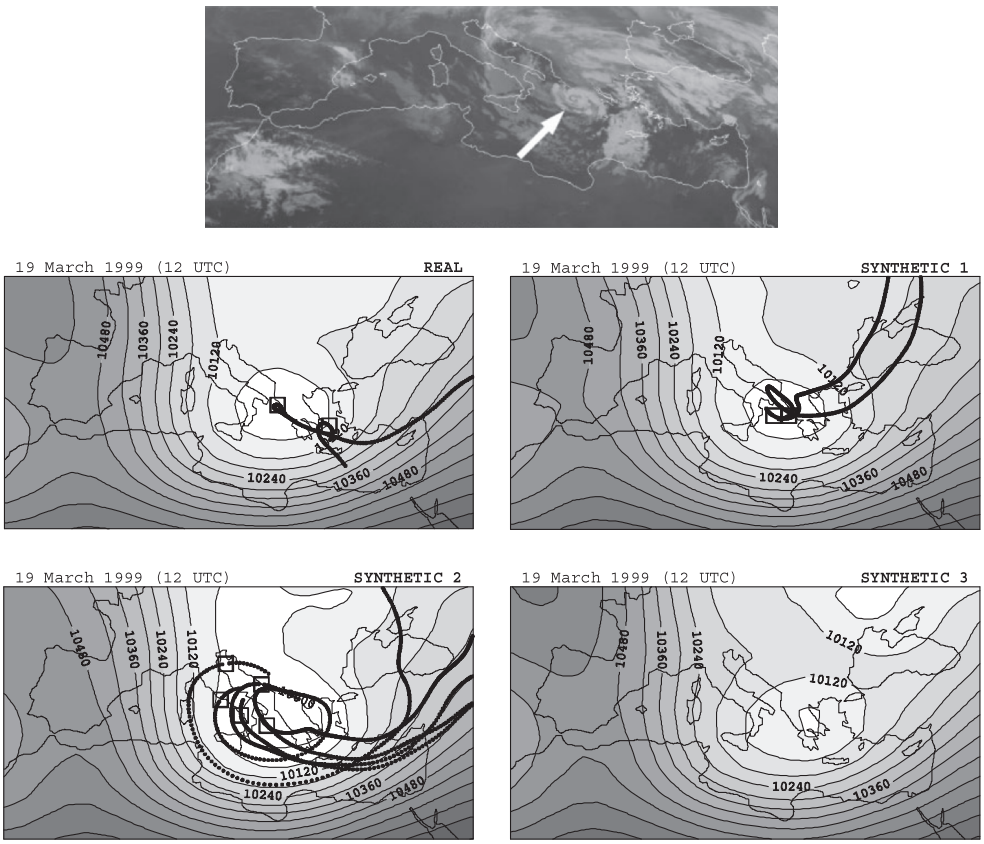

Figure 4. Analysis of the synoptic scenario associated with the medicane of 19 March 1999 (the upper panel indicates the position of the storm at 18:00 UTC). It is shown the geopotential height at 250 hPa (contour interval 60 gpm) extracted from the ERA-40 reanalysis at 12:00 UTC (REAL) and from three synthetically generated analogs (SYNTHETIC 1, 2, and 3). For each case, potential tracks identified during the episode according to the method described in the text are indicated (note that SYNTHETIC 3 did not produce tracks).

2.2. Mediterranean Specificities

[7] Unfortunately, the same statistical-deterministic technique cannot be applied directly to the Mediterranean. First, the history of medicane genesis is far too sparse to form a reasonable probability distribution of genesis. Second, the monthly climatological mean potential intensity is inadequate for generating synthetic medicanes, because such storms appear only to develop under conditions that depart quite far from climatology. Indeed, synoptic and numerical analyses of a few well-known cases show that an inevitable precursor of these storms is the approach, or development in situ, of a deep, cutoff, cold-core cyclone in the upper and middle troposphere [*Emanuel*, 2005b; *Tous and Romero*, 2012]. Such a meteorological scenario does not admit the separation of time scales made over the tropics between the synthetic wind field (characterized by a fast scale) and the thermodynamical environment found along the tracks (a slow-varying property). Dynamical and thermodynamical factors appear strongly interlinked and evolve in close conjunction with the movement, growth, and decay of midlatitude weather systems. These characteristic modes of interrelation and organization of the fields in space and time should dictate our adapted method for the synthetic generation of tracks. On the other hand, application of some reasonable criteria for the detection of good candidates among these tracks, in terms of the potential genesis of a medicane, seems to be also necessary. (We could of course attempt to simulate a countless collection of unfiltered tracks (e.g., randomly distributed over the maritime areas), but the computational burden necessary before producing a sufficient number of medicanes would make this exercise very inefficient.)

2.3. Description of the New Method

[8] The generation of synthetic medicanes demands a redesign of the original method with regard to the production of physically sound trajectories and concomitant kinematic and thermodynamical environments. Here we introduce a new method in which the spatial and temporal variability at synoptic scale of key ingredients for the environmental control of these storms that are needed by the intensity model (potential intensity, midtropospheric temperature and humidity, and winds in the lower and upper troposphere) is converted via principal component analysis (PCA) into a new space represented by the resulting independent principal components (PCs). This decomposition is performed for each month separately to better encompass the marked annual cycle of the

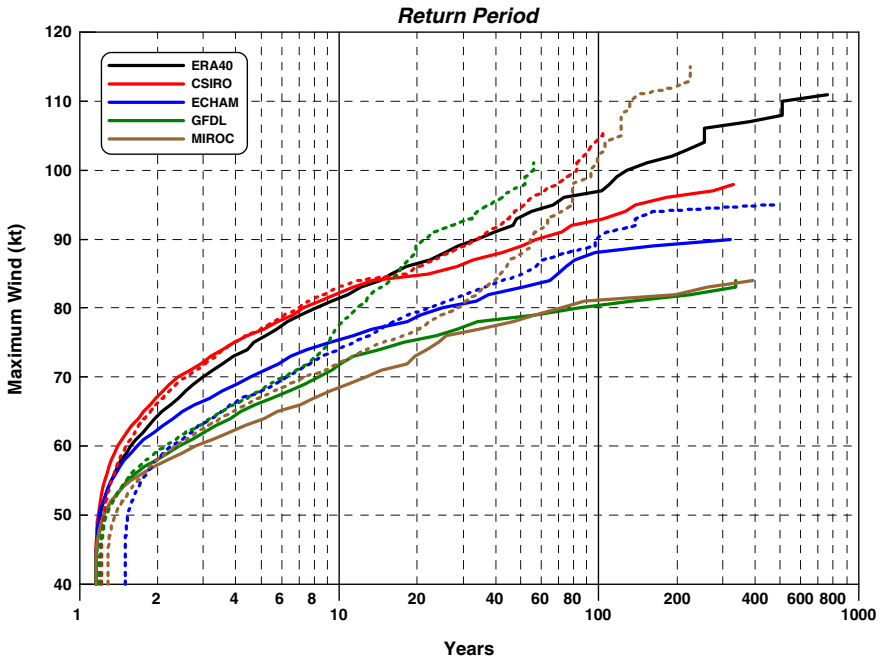

Figure 5. Return period (horizontal axis, in years) of medicanes according to the maximum wind induced at the surface (vertical axis, in knots). Continuous lines refer to the current climate and dashed lines to the future climate, following the color coding indicated in the legend.

Mediterranean region and is implemented in two sequential steps using daily gridded fields of *PI*, temperature, and relative humidity at 600 hPa and geopotential heights at 850 and 250 hPa (as surrogates of the winds via the geostrophic relation) extended over the geographical domain shown in Figure 8. First, we account for the existing correlations in space and, simultaneously, among the fields (i.e., correlations between all possible pairs of time series pertaining to the same or different physical variables) and subject the corresponding spatial-field correlation matrix to PCA. These correlations are so prominent that with only 10 PCs it is possible to account for about 70% of the variance in the data, although we systematically retain all PCs to avoid missing any "small-scale" meteorological structure explicitly resolved in the reanalysis or GCM coarse fields. We can refer to these PCs as spatial-physical PCs. By definition, any given set of these PCs would result in a physically meaningful daily state since it would express a proper linear combination of the spatial and intervariable modes of

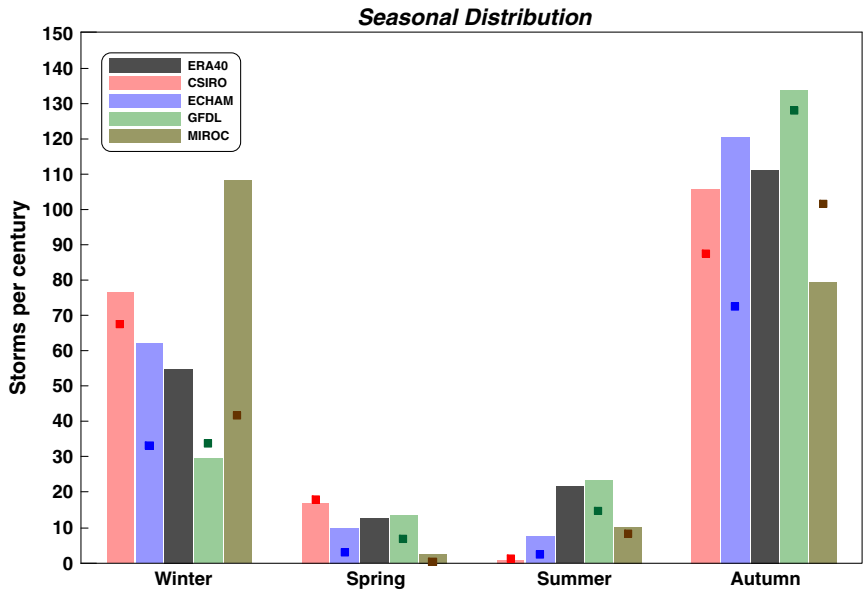

Figure 6. Seasonal distribution of medicanes. Color bars refer to the current climate as indicated in the legend, and bold squares refer to the future climate for the four GCMs analyzed.

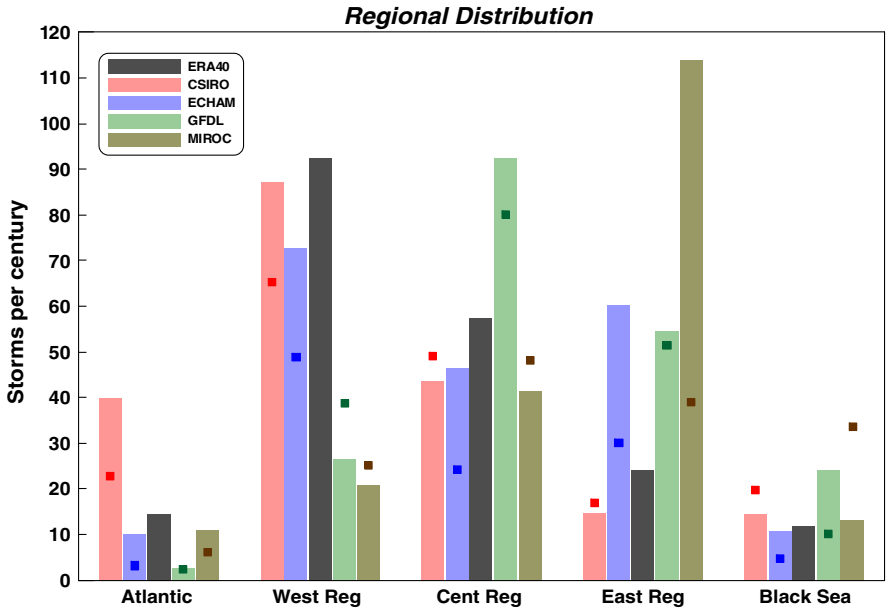

Figure 7. As in Figure 6 but for the regional distribution of medicane genesis locations. These regions are indicated in the bottom panel of Figure 8.

variation found in the climatic data (see an example of these modes for the first PC in Figure 2), but this would not solve the problem of the temporal evolution of the states. Therefore, we account for the temporal structure of the data in a second step, where the matrix of the time-lagged correlations among the previous spatial-physical PCs is subjected to a new PCA. For these correlations, we consider a time window up to 10 days (enough to comprise any synoptic-scale evolution over the considered region), and we can refer to the resulting PCs as temporal PCs. Again, we retain all these PCs. These temporal PCs, with mean 0 and standard deviation 1, very nicely tend to follow a Gaussian distribution, and therefore their probabilities can be easily analytically described (Figure 3).

[9] By construction, random draws from the fitted probability distribution of these independent temporal PCs, once converted back into physical space via the intermediate spatial-physical PCs, are tantamount to generating 10 day sequences of spatiotemporally coherent fields compatible with the observed climate, which also respect the mutual covariances among the environmental fields. Nevertheless, we are not so permissive in our final method, and, instead, observed states (i.e., observed combinations of temporal PCs) are first randomly selected from the data and then slightly perturbed in each temporal PC. These positive or negative perturbations are independent for each PC and randomly defined according to a normal distribution of standard deviation 0.25 (see Figure 3). The final result of the method is thus the production of synoptic evolutions that behave as analogs of locations actually visited in the climate phase space.

[10] The synthetic 10 day climate realizations are scrutinized for the potential incubation of medicanes based on the presence of high values of an empirical index of genesis that have been shown to accompany—as a necessary but not sufficient ingredient—the development of real events [*Tous and Romero*, 2012]. This index was formulated by *Emanuel and Nolan* [2004] in the context of tropical cyclone research:

$$GEN = \left(10^5\eta\right)^{3/2}\left(\frac{RH}{50}\right)^3\left(\frac{PI}{70}\right)^3\left(1+0.1V_{\text{shear}}\right)^{-2} \qquad (2)$$

and depends on potential intensity (PI), absolute vorticity at low levels (η), midtropospheric relative humidity (RH), and vertical wind shear across the troposphere (V_{shear}). The GEN index summarizes the essence of the medicane-prone environments established over the Mediterranean Sea when a large-scale baroclinic system, maturing into a cold cutoff low at midtropospheric to upper-tropospheric levels, approaches or develops in situ. In these circumstances, the air through a deep layer of the troposphere is lifted through large vertical displacements, cooling it and increasing its relative humidity. Such an atmosphere is susceptible to tropical cyclone-like development for several reasons: first, the local thermodynamic potential for tropical cyclones is large according to (1), owing to the anomalously large air-sea thermodynamic disequilibrium; the air through a deep column is very humid, inhibiting the formation of convective downdrafts that tend to prevent this kind of cyclogenesis; and the wind shear—both directional and in magnitude—will not be large under this mature synoptic scenario. Note that all these ingredients favor high values of GEN according to expression (2).

[11] Based on the GEN spatial distribution computed from the synthetic daily fields, a possible medicane genesis is implied when, within a cyclonic environment ($\eta > 10^{-4}\,\text{s}^{-1}$), we observe a local maximum of GEN exceeding 20 units. When a potential genesis event is detected, a candidate track is built from its location using the Beta and Advection Model, integrated 6 h backward in time (in order to account for the preexisting conditions) and several days forward in time, with a time step of 30 min. The meteorological

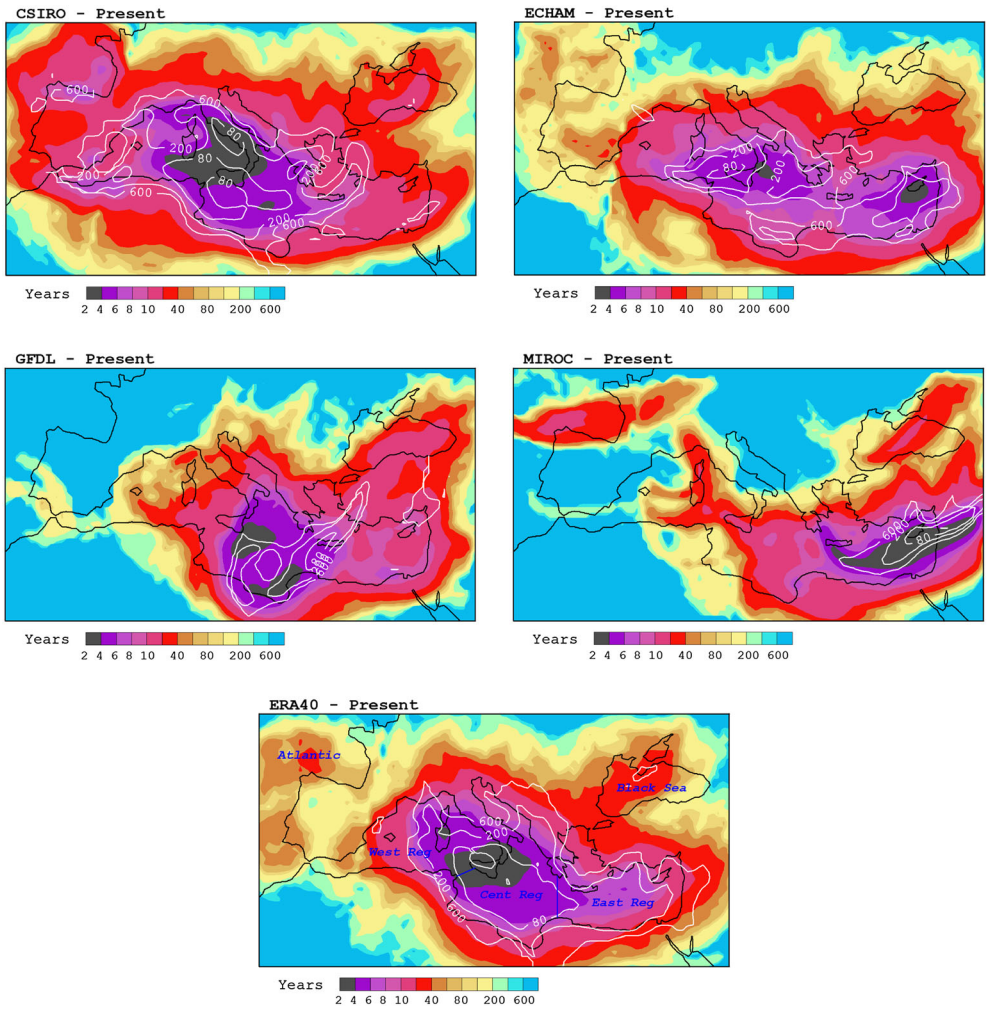

Figure 8. Return periods for the present climate of medicane surface winds above 34 kt (color) and 60 kt (white contours, for the values shown in the color scale). The bottom panel also indicates the maritime regions discussed in the text (blue).

parameters, bathymetry, and ocean mixed layer depth necessary for the atmospheric-oceanic numerical model simulations are obtained by interpolation along the track points.

2.4. An Example

[12] The ability of the *GEN*-based criteria to capture the medicane potential of upper-tropospheric cold-core lows was tested on known episodes of medicanes from *Tous and Romero* [2012] using the ERA40 reanalyses. The method invariably indicated one or several potential tracks within these scenarios (see an example for the medicane of March 1999 in Figure 4). This example also illustrates the effects of the randomly built synoptic analogs on the number and position of trajectories. An open question when more than one track is inferred is whether we should limit the subsequent atmospheric-oceanic model simulation to a single track (e.g., the one exhibiting the largest accumulated values of *GEN* along its path), but here we interpret the number of tracks as another indicator of the probability of genesis offered by a particular environment, and since we are pursuing a statistical depiction of the medicane risk, not the analysis of individual case studies, we simulate all of them.

3. Medicanes in the Present and Future Climates

3.1. Experiments

[13] Many thousands of climate realizations were generated using the aforementioned technique for each month of the year based on daily data from the ERA40 reanalysis [*Uppala et al.*, 2005] and the output from four different "Coupled Model Intercomparison Project" (CMIP3) GCMs run under the SRES A2 [*Intergovernmental Panel on Climate Change*, 2000] emission scenario: CSIRO Mk3.0 [*Cai et al.*, 2003], ECHAM 5 [*Cubasch et al.*, 1997], GFDL CM2.1 [*Manabe et al.*, 1991], and MIROC 3.2 [*Hasumi and Emori*, 2004]. The horizontal resolution of these GCMs ranges from 1.9° to 2.8° depending on the model; for consistency, we used the ERA40 reanalyses at a resolution of 2.5°. As representative of the current and future climate conditions, the periods 1981–2000 and 2081–2100 have been chosen from these data sets.

[14] Around 15,000 candidate tracks were synthetically generated for the ERA40 and GCM climates of the baseline period. The frequency of successful storms (i.e., storm tracks exhibiting intensification to at least tropical storm force winds of 34 kt or 63 km/h) was about 10–20%, and these absolute frequencies were normalized in each case to the

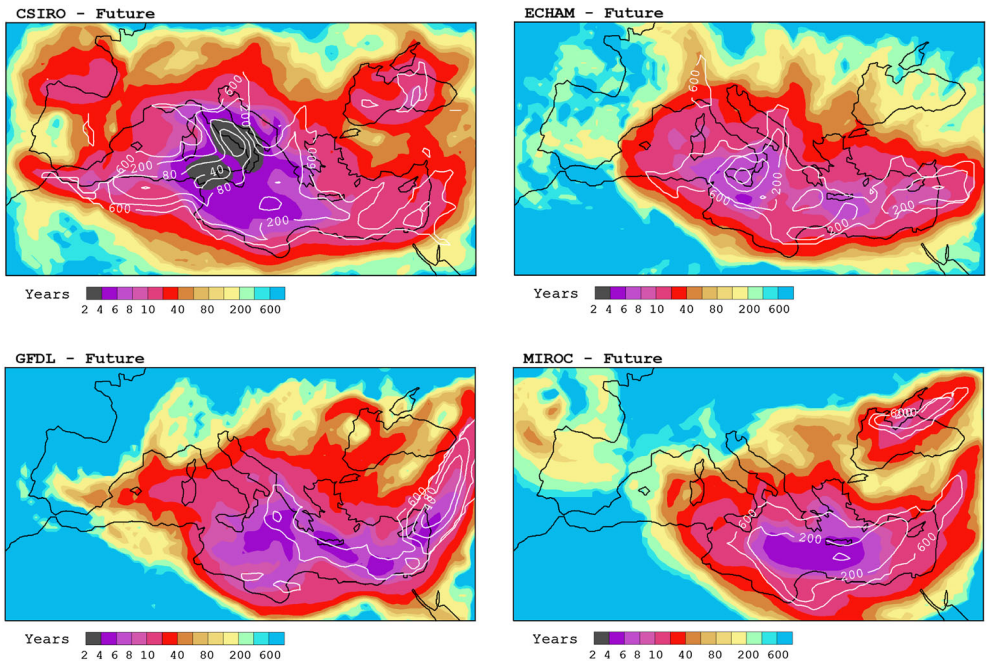

Figure 9. As in Figure 8 but for return periods corresponding to the future climate.

"observed" rate of two storms per year. (Such a normalization is necessary because the initial random seeding rate is arbitrary.) Finally, candidate tracks were generated and simulated for the future period of each GCM based on the same number of 10 day realizations that was used for the current climate, and the frequency of simulated medicanes normalized in proportion. It should be noted that the statistical products shown in the next section (e.g., return periods) were calculated using the full set of simulated successful storms (i.e., several thousands), as if we were dealing with large samples of events occurring through the centuries in a "frozen" climate; the effects of the frequency normalization on these products is a simple rescaling of the calculated values.

3.2. Results

[15] The four analyzed models all indicate a reduced frequency of medicanes by the late 21st century: the current long-term risk of 200 storms per century decreases to 183, 174, 152, and 111 storms according to GFDL, CSIRO, MIROC and ECHAM future climates, respectively. Interestingly, the projection made in *Cavicchia* [2013] using a dynamical downscaling of the ECHAM climate revealed a similar reduction of about 40% in the future incidence of medicanes. In spite of the projected shrinkage in the number of medicanes, the models systematically produce a higher number of violent storms, i.e., with maximum surface winds greater than 80 kt. This change in the intensity distribution is nicely illustrated in Figure 5 as an upward deflection of the future return period curves beyond the 10 year coordinate. Since the four analyzed GCMs seem to be underestimating the maximum intensity of storms in the current climate (i.e., model curves lie below the ERA40 reference plot in Figure 5), the expected increase in the future incidence of severe medicanes could be even worse than numerically predicted.

[16] Documented cases of medicanes [e.g., *Tous and Romero*, 2012] show that this phenomenon is most frequent in the cold season and in the western and central basins of the Mediterranean. Such seasonal and subregional patterns are confirmed in the distributions of ERA40-derived synthetic storms, shown as dark gray in the bar charts of Figures 6 and 7. Autumn incidence is double the frequency of winter storms, and very few cases occur in the warm season, while there is a linear decreasing trend in the genesis of storms from west to east in the Mediterranean, and hardly 10 cases per century can be expected over the Atlantic sector and Black Sea. Clearly, the cold air intrusions from higher latitudes that tend to occur over the west-central Mediterranean in the cold season are the ideal circumstances for building the thermodynamic disequilibrium between the sea and the atmosphere needed by medicanes, even in the winter period when sea surface temperatures can be as low as 14–15°C.

[17] The ability of the GCMs to reproduce for the baseline period the previous seasonal and regional distributions is a crucial test for the models, since the only type of calibration applied in our method was for the total number of storms. The annual cycle is reasonably well captured by the models except by MIROC, which exhibits its maximum in winter instead of autumn (Figure 6). The projected loss of storms would affect the four seasons of the year, in such a way that the seasonal distribution is not expected to change in the future in relative terms. Again, MIROC seems to be an exception to the general rule, showing an appreciable loss of events in winter but a significant gain in autumn. Regarding the subregional distributions (Figure 7), the projections seem to be more uncertain and some of the individual results for the current climate even problematic. In comparison with ERA40, the best results are obtained with CSIRO and ECHAM models, although they tend to overemphasize the Atlantic and Eastern-Region storms, respectively. GFDL underestimates the frequency of medicanes in the western regions in favor of the central and eastern regions. Another anomalous behavior is that of

MIROC, which unrealistically prioritizes the Eastern-Region events to the detriment of the western Mediterranean storms.

[18] Finally, Figures 8 and 9 summarize the wind risk associated with medicanes under present and future climatic conditions. This risk is expressed by means of the calculated return periods of tropical storm force surface winds (1 min average greater than 34 kt) and also of surface winds above 60 kt (i.e., roughly hurricane-force speeds). The bottom panel of Figure 8 confirms our current understanding of the medicane phenomenology: these storms more often affect the islands and coasts of the western and central basins than elsewhere among the populated areas of the Mediterranean. The maximum 34 kt risk (i.e., lowest return periods) regions are found around Sicily and south of the Italian peninsula. Return periods of violent winds of 60 kt and greater, average around a few centuries in much of the Mediterranean basin and attain values less than a century over southern Italy, Sicily, and nearby maritime areas. The general spatial pattern of the risk is well captured by CSIRO and ECHAM for both wind thresholds, although with a certain tendency to overemphasize medicane activity westward in the former model and eastward in the latter. Compared to ERA40, the simulated highest wind risk based on GFDL is shifted somewhat eastward and mostly focused on the central region. As already discussed, MIROC produces too many tracks in the eastern region and too few in the central and western basins (Figure 8). It should be noted that slight or even severe discrepancies of GCM-based products at subregional scales are a known limitation of these tools, including their applications to hurricane risk assessment [e.g., *Emanuel et al*., 2008].

[19] The lower frequency of storms projected for the future is evident in the risk of medicane winds (compare Figure 9 versus Figure 8 for the 34 kt category): there is a general increase in future return periods for the four GCMs. Regarding the spatial pattern of the risk, this pattern is only slightly changed in the most reliable models at subregional scales (CSIRO and ECHAM), while there is a future tendency to spread medicane risk toward the east in GFDL and to shift it toward the central Mediterranean in MIROC. In spite of the expected decrease in the future occurrence of tropical storm force winds, the areal extent of the risk of violent winds (say 60 kt events, Figure 9, and higher extremes, not shown) is maintained or increased in all future climates, again in agreement with the statistics shown in Figure 5.

4. Implications

[20] This work adapted for the Mediterranean region our statistical-deterministic approach to hurricane risk assessment, with the aim of assessing medicane risk under current and future climate conditions. The new method is a good alternative to computationally expensive classical methods (e.g., dynamical downscaling of storms), with the extra benefit of producing statistically large populations of events.

[21] We produced unprecedented wind risk maps for the Mediterranean region, in general agreement with the "known" phenomenology of medicanes in the current climate as derived from the few documented cases: these rare but extreme storms show their maximum incidence in the cold season and over the central Mediterranean region. A similar spatial-temporal signal can be inferred from the few existing exercises of dynamical downscaling of medicanes, and our own dynamical projections for the future seem to agree with the general trends in medicane distribution and intensity found in this work. Nevertheless, a thorough comparison for the problem of dynamical downscaling and statistical-deterministic techniques is a pending task. We are also planning an extension of this work to the most recent generation CMIP5 climate models and a wider choice of models and emission scenarios in order to better resolve the uncertainties that affect medicane risk assessment, especially at subregional scale.

[22] In spite of these geographical uncertainties, the GCMs analyzed in this work consistently project fewer medicanes at the end of the century compared to present (about 10–40% less) but indicate a higher number of violent cases. As the production of wind energy—and thus the power of destruction—of these storms is proportional to the wind speed cubed, we see our findings as a cause of future concern for exposed Mediterranean societies.

[23] **Acknowledgments.** The authors thank the ECMWF and the WCRP CMIP3 multimodel database for providing access to the ERA40 reanalysis and GCM simulations. This research was supported by the MEDICANES (CGL2008-01271) and PREDIMED (CGL2011-24458) projects, and the leading author visited MIT under Grant PR2011-0276. These actions were funded by the Spanish "Ministerio de Ciencia e Innovación" and "Ministerio de Educación," respectively.

References

Cai, W., M. A. Collier, P. D. Durack, H. B. Gordon, A. C. Hirst, S. P. O'Farrell, and P. H. Whetton (2003), The response of climate variability and mean state to climate change: Preliminary results from the CSIRO Mark 3 coupled model, *CLIVAR Exchanges*, *28*, 8–11.

Cavicchia, L. (2013), A long-term climatology of medicanes. PhD Thesis, 121 pp. (Available from Ca' Foscari University of Venice).

Cubasch, U., R. Voss, G. Hegerl, J. Waskiewitz, and T. Crowley (1997), Simulation of the influence of solar radiation variations on the global climate with an ocean-atmosphere general circulation model, *Clim. Dynam.*, *13*, 757–767.

Emanuel, K. (1986), An air-sea interaction theory of tropical cyclones. Part I: Steady-state maintenance, *J. Atmos. Sci.*, *43*, 585–604.

Emanuel, K. (1987), The dependence of hurricane intensity on climate, *Nature*, *326*, 483–485.

Emanuel, K. (1995), The behavior of a simple hurricane model using a convective scheme based on subcloud-layer entropy equilibrium, *J. Atmos. Sci.*, *52*, 3959–3968.

Emanuel, K. (2005a), Increasing destructiveness of tropical cyclones over the past 30 years, *Nature*, *436*, 686–688.

Emanuel, K. (2005b), Genesis and maintenance of Mediterranean hurricanes, *Adv. Geosc. 2*, 217–220.

Emanuel, K. (2006), Climate and tropical cyclone activity: A new model downscaling approach, *J. Climate*, *19*, 4797–4802.

Emanuel, K., and D. Nolan (2004), Tropical cyclone activity and the global climate system, paper presented at 26th Conference on Hurricanes and Tropical Meteorology, Amer. Meteor. Soc., Miami, Fla, 240–241.

Emanuel, K., S. Ravela, E. Vivant, and C. A. Risi (2006), Statistical-deterministic approach to hurricane risk assessment, *Bull. Amer. Meteor. Soc.*, *87*, 299–314.

Emanuel, K., R. Sundararajan, and J. Williams (2008), Hurricanes and global warming: Results from downscaling IPCC AR4 simulations, *Bull. Amer. Meteor. Soc.*, *89*, 347–367.

Ernst, J. A., and M. A. Matson (1983), Mediterranean tropical storm?, *Weather*, *38*, 332–337.

Fita, L., R. Romero, A. Luque, K. Emanuel, and C. Ramis (2007), Analysis of the environments of seven Mediterranean tropical-like storms using an axisymmetric, nonhydrostatic, cloud resolving model, *Nat. Hazards Earth Syst. Sci.*, *7*, 1–16.

Frei, C., and C. Schär (2001), Detection of probability of trends in rare events: Theory and application to heavy precipitation in the Alpine region, *J. Clim.*, *14*, 1568–1584.

Gaertner, M. A., D. Jacob, V. Gil, M. Domínguez, E. Padorno, E. Sánchez, and M. Castro (2007), Tropical cyclones over the Mediterranean Sea in climate change simulations, *Geophys. Res. Lett.*, *34*, L14711, doi:10.1029/2007GL029977.

Hasumi, H., and S. Emori (Eds.) (2004), *K-1 Coupled GCM (MIROC) Description K-1 Tech. Rep.*, 1, pp. 34, Cent. for Clim. Syst. Res., Univ of Tokyo, Tokyo.

Henderson-Sellers, A., et al. (1998), Tropical cyclones and global climate change: A post-IPCC assessment, *Bull. Amer. Meteor. Soc.*, *79*, 9–38.

Homar, V., R. Romero, D. J. Stensrud, C. Ramis, and S. Alonso (2003), Numerical diagnosis of a small, quasi-tropical cyclone over the western Mediterranean: Dynamical vs. boundary factors, *Quart. J. R. Meteorol. Soc.*, *129*, 1469–1490.

IPCC (2000), *Special Report on Emissions Scenarios*, edited by N. Nakicenovic and R. Swart, Cambridge Univ. Press, Cambridge (UK), pp. 570.

Klein Tank, A. M. G., and G. P. Können (2003), Trends in indices of daily temperature and precipitation extremes in Europe, 1946–1999, *J. Clim.*, *16*, 3665–3680.

Knutson, T., and R. Tuleya (2004), Impact of CO_2-induced warming on simulated hurricane intensity and precipitation: Sensitivity to the choice of climate model and convective parameterization, *J. Climate*, *17*, 3477–3495.

Lagouvardos, K., V. Kotroni, S. Nickovic, D. Jovic, and G. Kallos (1999), Observations and model simulations of a winter sub-synoptic vortex over the central Mediterranean, *Meteorol. Appl.*, *6*, 371–383.

Lighthill, J., G. Holland, W. M. Gray, C. Landsea, G. Craig, J. Evans, Y. Kurihara, and C. P. Guard (1994), Global climate change and tropical cyclones, *Bull. Amer. Meteor. Soc.*, *75*, 2147–2157.

Manabe, S., J. Stouffer, M. J. Spelman, and K. Bryan (1991), Transient responses of a coupled ocean-atmosphere model to gradual changes of atmospheric CO_2. Part I: Mean annual response, *J. Clim.*, *4*, 785–818.

Marks, D. G. (1992), *The Beta and Advection Model for Hurricane Track Forecasting*, NOAA Tech. Memo. NWS NMC 70, pp. 89, National Oceanic and Atmospheric Administration (NOAA), Washington DC.

Moscatello, A., M. M. Miglieta, and R. Rotunno (2008), Observational analysis of a Mediterranean 'hurricane' over south-eastern Italy, *Weather*, *63*, 306–311.

Rasmussen, E., and C. Zick (1987), A subsynoptic vortex over the Mediterranean sea with some resemblance to polar lows, *Tellus*, *39*, 408–425.

Reale, O., and R. Atlas (2001), Tropical cyclone-like vortices in the extratropics: Observational evidence and synoptic analysis, *Weather Forecast.*, *16*, 7–34.

Royer, J. F., F. Chauvin, B. Timbal, P. Araspin, and D. Grimal (1998), A GCM study of impact of greenhouse gas increase on the frequency of occurrence of tropical cyclones, *Climate Dyn.*, *38*, 307–343.

Sugi, M., A. Noda, and N. Sato (2002), Influence of the global warming on tropical cyclone climatology: An experiment with the JMA global model, *J. Meteor. Soc. Japan*, *80*, 249–272.

Tous, M., and R. Romero (2012), Meteorological environments associated with medicane development, *Int. J. Climatol.*, doi:10.1002/joc.3428.

Tous, M., R. Romero, and C. Ramis (2012), Surface heat fluxes influence on medicane trajectories and intensification, *Atmos. Res.*, doi:10.1016/j.atmosres.2012.05.022.

Uppala, S. M., et al. (2005), The ERA-40 re-analysis, *Q. J. R. Meteorol. Soc.*, *131*, 2961–3012, doi:10.1256/qj.04.176.

Webster, P. J., G. J. Holland, J. A. Curry, and H. R. Chang (2005), Changes in tropical cyclone number, duration and intensity in a warming environment, *Science*, *309*, 1844–1846.